Transpiration from canopy temperature: Implications for the assessment of crop yield in almond orchards

V. Gonzalez-Dugo[a],[*], M. Lopez-Lopez[a], M. Espadafor[b], F. Orgaz[a], L. Testi[a], P. Zarco-Tejada[a], I.J. Lorite[b], E. Fereres[a],[c]

[a] Instituto de Agricultura Sostenible (IAS), Consejo Superior de Investigaciones Científicas (CSIC), Alameda del Obispo s/n, 14004 Cordoba, Spain
[b] IFAPA – Centro Alameda del Obispo, Junta de Andalucia, Alameda del Obispo s/n, 14004 Cordoba, Spain
[c] Department of Agronomy, University of Cordoba, Campus Universitario de Rabanales, 14014, Cordoba, Spain

ABSTRACT

This paper evaluates the usefulness of the Crop Water Stress Index (CWSI) for monitoring transpiration and water status in almond trees, and proposes a methodology for assessing crop yield derived from the relation between canopy temperature and transpiration. For this purpose, a Non-Water Stress Baseline (NWSB) was developed from canopy temperature measurements taken with Infrared Thermometers (IRT) installed permanently over well-watered trees for three years. Tree transpiration was measured continuously with sap flow probes installed in the same trees than the IRT sensors. The calculated CWSI was closely related to water potential and stomatal conductance measured during kernel filling, as well as with transpiration and the ratio kT/GC (the transpiration coefficient over the ground cover). Taking into consideration this relation and the water production function recently published, the seasonal CWSI was compared to final yield and the regression yielded good results ($R^2 = 0.80$). An empirical relationship between the CWSI acquired remotely from two flights performed during the kernel filling stage and crop yield was determined for this orchard. The estimated yield from the proposed methodology was compared to ground-truth measurements of crop yield measured in 80 trees during 2014 and 2015. The result obtained a RMSE that yielded 1.54 kg/tree. This study thus demonstrates that CWSI is closely related to the transpiration and the ratio kT/GC. This relation settles the basis for the development of methodologies for estimating water-limited crop yield from thermal derived information.

1. Introduction

Irrigation management is one of the main issues that almond growers' must deal with. Almond cultivation in Spain has traditionally taken place under low-input, rainfed conditions in marginal soils, but this situation is now quickly shifting towards more intensive production systems grown in suitable soils and under irrigation. This is a consequence of the high prices fetched by this commodity in recent years, leading to the establishment of new almond orchards in many Spanish irrigation schemes. The lack of information about crop water needs and on the responses to irrigation has been addressed in several studies conducted in Spain using the hard-shell cultivars typically grown in Europe (Romero et al., 2004; Egea et al., 2010; Espadafor et al., 2017; López-López et al., 2018a). These works have increased the knowledge about the best practices to manage irrigation under the semiarid conditions of the Mediterranean area. The successful application of the strategies outlined in these studies relies on the accurate assessment of

orchard water status. It remains thus essential to develop tools and indicators enabling the monitoring of water status of almond orchards.

The use of thermal information to determine crop water status has increased in recent decades (Jones et al., 2002). Water stress induces stomatal closure, reduces evaporative cooling and increases leaf temperature (Hsiao, 1973). The main advantage of using canopy temperature, compared to traditional measures to assess crop water status, are the remote and non-destructive acquisition and the reliability. Moreover, it allows the assessment of large areas in short time periods when the canopies are sensed from aerial vehicles (Gonzalez-Dugo et al., 2013). However, the spatial resolution of the measures limits the use of thermal data from satellites in orchards, a limitation that has been overcome installing sensors in manned or unmanned aerial vehicles (UAVs). The widespread development of UAVs for commercial purposes has boosted the availability of this information for research and commercial purposes. Different types of cameras may be installed on UAVs which fly over agricultural fields and provide information that

can be related to crop physiological status (Berni et al., 2009; Zarco-Tejada et al., 2012; Turner et al., 2012). Even though this service is now available and offered by private companies, there are still gaps in our knowledge that prevent the establishment of a standard methodology for monitoring water needs and for scheduling irrigation based on thermal information. The main limitation to actual knowledge is related to the efficient use of thermal information and its translation to actual irrigation requirements, although some promising results were recently published (O'Shaughnessy et al., 2017).

The influence of evaporative demand on canopy temperature via air temperature and the vapor pressure deficit requires its normalization, for comparative purposes. This normalization can be carried out using the Crop Water Stress Index (CWSI) developed by Idso, Jackson and coworkers (Idso et al., 1981; Jackson et al., 1981). Empirical and theoretical approaches have been proposed to calculate the CWSI (Maes and Steppe, 2012). The empirical approach is often proposed because of the low input requirements, once the baselines have been established for a given crop and climatic conditions. The Non-Water Stress Baseline (NWSB) determines the lower limit for the CWSI calculation and can be empirically determined by regressing the difference of canopy and air temperature (Tc-Ta) against the vapor pressure deficit (VPD) on clear sunny days under well-watered conditions, both obtained around midday. According to the methodology developed by Idso et al. (1981), the NWSB for a given crop, together with the actual canopy temperature and the hourly weather data from a meteorological station is sufficient for calculating the CWSI. This approach, originally developed for herbaceous crops, has already been adapted to the most important Mediterranean tree crops, such as citrus (Gonzalez-Dugo et al., 2014), pistachio (Testi et al., 2008), olive (Egea et al., 2017), peach (Bellvert et al., 2016a) and vines (Bellvert et al., 2016b), among others. One requirement for obtaining a robust procedure for determining the CWSI in tree crops is the need to rely on a long-term series of temperature readings (at least two years), given the tendency for alternate bearing in these crops and the observed variations in tree transpiration associated with fruit load (López-López et al., 2018a).

Crop yield is often limited by water availability (Tanner and Sinclair, 1983). There is a close link between these two terms that are related by means of the water productivity. In orchard tree crops, the water productivity is not constant, and vary according to the level of water stress reached by the crop and the phenological moment affected by the water shortage, as there is contrasted sensitivity to water stress during the season (Fereres et al., 2012). This is the base of the development of the strategy termed regulated deficit irrigation (RDI). It consists on the application of water stress during certain periods that are least sensitive to water stress (Fereres and Soriano, 2007). As a result, water applied is reduced without a penalty in crop yield; thus, water productivity increases. In almond, several studies have demonstrated that kernel unit weight is strongly affected by water stress applied during kernel filling period (Goldhamer and Fereres, 2017; Naor et al., 2017; López-López et al., 2018b). Taking this into account, it can be anticipated that the accurate assessment of crop water status during pre-harvest can be useful for monitoring crop yield in semiarid conditions. The working hypothesis is thus that it is possible to develop a methodology for monitoring almond water status and yield based on high-resolution airborne canopy temperature measurements and their relationship with transpiration rate. This work was thus aimed at: i) developing a reliable NWSB for almond under Mediterranean, semiarid conditions, ii) establishing the CWSI as a suitable index for monitoring almond water status and water use under these conditions, and iii) developing a methodology for predicting crop yield, based on the close relationship between transpiration rate and CWSI with yield during the pre-harvest period.

2. Materials and methods

2.1. Site description and experimental design

The experiment was carried out for three years (from 2014 to 2016) in a 5.5-ha experimental almond orchard at the Research Centre of IFAPA - Alameda del Obispo, Cordoba Spain (37°52′N, 4°49′W). The almond orchard (cv. *Guara*, grafted onto the GF-677 rootstock) was planted in 2009 in a 6 x 7 m grid (238 trees/ha) on a sandy loam soil. The climate in the area is Mediterranean, characterized by warm and dry summers and cold and wet winters, with an annual rainfall and reference evapotranspiration (ETo; Penman-Monteith) around 550 and 1300 mm, respectively.

Five treatments were compared in a randomized block design with four replicates per treatment. Each individual plot comprised 16 trees (four rows and four trees per row), the central four being monitored. Trees were daily irrigated with two laterals per tree row, with 12 emitters ($4\,l\cdot h^{-1}$) per tree. In Control treatment (C), irrigation was applied according to full crop requirements. Full requirements were calculated according to the estimated crop evapotranspiration, calculated following Fereres et al. (2012), using a reduction coefficient based on canopy size. The severe regulated deficit irrigation treatment (RDIs) consisted on supplying only 15% of the control treatment during kernel-filling stage in 2014, while in 2015 and 2016 20% of the control water was applied. RDIs trees were rewatered after harvest with 60% of control. The moderate regulated deficit irrigation (RDIm) applied 40% of control treatment and received the same water as the control after harvest. In the sustained deficit irrigation treatment (SDI), water application was reduced to 75% of the control throughout the season. Finally, the fifth treatment (RDIs,n) had the same schedule as RDIs, but the nitrogen application was also reduced to 75% in relation to control treatment. Each treatment was replicated four times. A single plot under rainfed conditions since 2013 was also included in the experimental design. This study was focused on control and RDIs treatment. The irrigation period lasted from DOY 69 to 278 in 2014, from 40 to 312 in 2015 and from 61 to 283 in 2016. For more information regarding the experimental site and treatments, see Espadafor et al. (2017) and López-López et al. (2018a). Weather data were obtained from an automatic weather station located about 300 m apart from the study site. The daily vapor pressure deficit (VPD; kPa) was calculated as the average value of hourly VPD, calculated using the air temperature and relative humidity.

2.2. Canopy temperature measurement and CWSI calculations

Four trees were instrumented with four infrared temperature (IRT) sensors with an angular field of view of 44° (Model IRR-P, Apogee Instrument Inc., Logan, Utah, USA) acquiring continuous crown temperature data from June 2014 to October 2016. Two trees of C treatment and two trees of RDIs were monitored, and their canopy temperatures were averaged to obtain an hourly value per treatment. Each sensor was installed on an aluminum mast 0.7 m above the canopy, targeting the crown in a 45° zenith angle and 0° azimuth (i.e., facing the canopy exposed to south), to ensure that pure and well illuminated vegetation fully covered the field of view. The accuracy of the sensor yielded ± 0.15 °C, according to the manufacturer. The sensors were connected to a datalogger that recorded the canopy temperature every minute and stored the 5-minute average. From DOY 192 to 203, 2016, a failure in electronics prevented data acquisition of canopy temperature.

The relationship between the vapor pressure deficit (VPD, kPa) and the difference between canopy and air temperature (Tc-Ta) for the well-irrigated trees (C treatment) was used to estimate the Non-Water Stress Baseline (NWSB). Only cloudless days were used for the calculation of the NWSB. The NWSB determined for values around midday (from 11 to 13 h, solar time) were used as lower limit to compute the Crop Water Stress Index (CWSI) according to Eq. 1:

$$CWSI = \frac{(Tc - Ta) - (Tc - Ta)_{LL}}{(Tc - Ta)_{UL} - (Tc - Ta)_{LL}} \tag{1}$$

Where $(Tc\text{-}Ta)_{LL}$ and $(Tc\text{-}Ta)_{UL}$ correspond to the lower and upper limit, respectively. The LL was calculated from the NWSB equation. The UL was obtained solving the NWSB equation for VPD = 0 then correcting for the difference in vapor pressure induced by the difference in temperature $Tc - Ta$ (Idso et al., 1981).

2.3. Sap flow measurements, water status and yield assessment

One tree from each treatment was monitored with two sap flow probes. The sensors were developed at the *Institute for Sustainable Agriculture* (CSIC, Spain) and are described in Testi and Villalobos (2009). The system uses the Compensation Heat Pulse (CHP) method, combined with the Calibrated Average Gradient (CAG) technique (Testi and Villalobos, 2009) when sap velocities are below $12\,\text{cm·h}^{-1}$. The probes measure the heat pulse velocity at four depths in the xylem, spaced 10 mm. The sensors were placed at 5, 15, 25 and 35 mm depth from the cambium. For more information about the calibration of the probes and the accuracy at estimating transpiration rate, see López-López et al. (2018b). The transpiration coefficient (kT) was calculated as the ratio of the daily transpiration rate (obtained from the sap flow probes) to the reference evapotranspiration (ETo). In order to normalize the transpiration by tree size, the ratio between the transpiration coefficient and ground cover (kT/GC) was determined.

Stem water potential and stomatal conductance were measured four to five times per year during the experiment. Stem water potential was measured with a pressure chamber (Soilmoisture Equipment Corp. model 3000, Santa Barbara, CA, USA) on two shaded leaves per tree located near the trunk and covered with aluminum foil for at least 30 min before the measurement. Stomatal conductance (Gs) was measured with a steady-state porometer (SC-1, Decagon Devices, Washington, DC, USA) on six sunlit leaves per tree.

Finally, at harvest, yield was assessed individually for every tree in the study. It comprised the central four trees per individual plot and the five treatments. As a result, 80 trees were harvested each year.

2.4. High-resolution aerial thermal imagery

A Cessna aircraft operated by the Laboratory for Research Methods in Quantitative Remote Sensing (QuantaLab), *Institute for Sustainable Agriculture* (IAS-CSIC, Spain), with a payload consisting on a thermal camera (FLIR SC655, FLIR Systems, Wilsonville, OR, USA) was flew at midday over the experimental site twice during 2014 (DOY 193 and 212) and 2015 (DOY 182 and 218). Flight height was 250 m above the ground, with the heading of the aircraft on the solar plane. The camera has a 640×480 pixel resolution with a 24.5 mm f1.0 lens, providing an angular FOV of $45 \times 33.7°$, which delivered a ground resolution of 25 cm (Fig. 1). The radiometric performance was validated in the laboratory using a black body (model P80 P, Land Instruments, Dronfield, UK), as was described in Berni et al. (2009) The thermal imagery was calibrated using ground temperature data collected with a handheld infrared thermometer (LaserSight, Optris, Germany) on each flight date. After calibration, the thermal imagery was mosaicked and ortho-rectified in order to get a single image for the whole scene. For more information about camera performance and calibration, see Zarco-Tejada et al. (2012).

Canopy temperature (*Tc*) for each tree of the experiment was extracted from the mosaic. An algorithm that applies a negative buffer was used to restrict the shape of the regions of interest considered and to exclude crown edges, thus avoiding soil/vegetation mixed pixels. Once the *Tc* of pure crowns was obtained, the CWSI at the object level was calculated after Eq. (1).
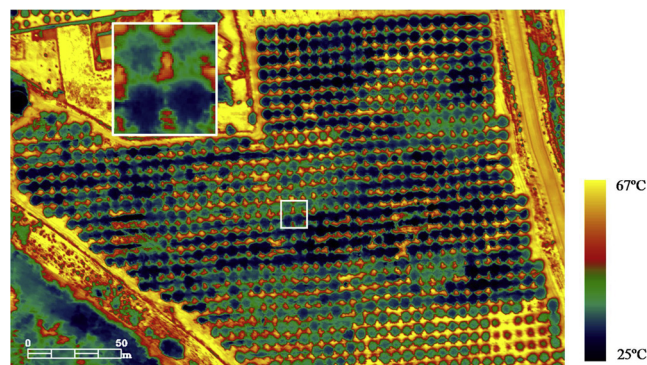

Fig. 1. Thermal image of the experimental site acquired on DOY 218 2015. Embedded in the top of the image, detail of the thermal imagery, showing the spatial resolution.

2.5. Data analysis

Statistical differences between the slope and the intercept for the non-water stress baselines (NWSB) were evaluated using the Comparison of Regression Lines tool included in the statistical software Statgraphics (Statsgraphic Centurion XVIII).

3. Results

The difference between canopy and air temperature (Tc-Ta) at noon in control trees oscillated between -2 and +2 °C (Fig. 2). For this time frame, the time evolution of Tc-Ta for the RDIs trees increased throughout the season, from values similar to control trees at the beginning of the stress period to reaching a maximum before rewatering, around +4 °C. For the RDIs treatment, a maximum value of +5.3 °C was recorded on DOY 207, 2015. Slight differences were observed in the pattern of stress development for the three years of the study. In 2014, RDIs trees maintained similar values to control until DOY 190. From this date, *Tc-Ta* increased in RDIs until reaching a maximum difference with control on DOY 220. For 2015 and 2016, differences between the two treatments started earlier and maintained a constant value close to 4 °C. Daily values of VPD were also plotted in Fig. 2. Values of VPD ranged from 0.6 to 4.2 kPa, and there were some differences in VPD patterns among the three study years (Fig. 2).

Values of *Tc-Ta* for control trees were regressed against VPD values from 9.00 to 17.00 solar time at 1-hour intervals (*data not shown*). As no differences were observed for the regressions obtained using data between 11.00 to 13.00, this time frame was selected to derive the NWSB and the results are presented in Fig. 3. The baseline did not differ among the three years (Fig. 3) and fitted the linear regression: *Tc-Ta* = −1.207·VPD + 3.419 (R^2 = 0.71).

Fig. 4 presents the calculated CWSI, using the methodology of Idso et al. (1981) to derive the upper limit for the CWSI. As expected, the control treatment showed CWSI values around 0. Values were slightly lower than 0 in 2016, possibly due to an increased transpiration, as was demonstrated in López-López et al. (2018a,b). The RDIs treatment displayed higher values than the control, approaching maximum values close to 1 near the end of the stress period, on DOY 215, 207 and 219 for 2014, 2015 and 2016, respectively.

The CWSI was closely related to the daily transpiration data obtained from the sap flow probes (Fig. 5). Data corresponding to values of CWSI below 0.05 have been discarded from this analysis, considering that, for that range, any change in the transpiration rate can be related to several factors other than water status, such as crop load or nutritional status, among others. The relationship adjusted to a negative linear regression with an R^2 of 0.79. For the selected range, the maximum transpiration rate was above 5 mm/day and corresponded to values of CWSI close to 0. The transpiration rate decreased until
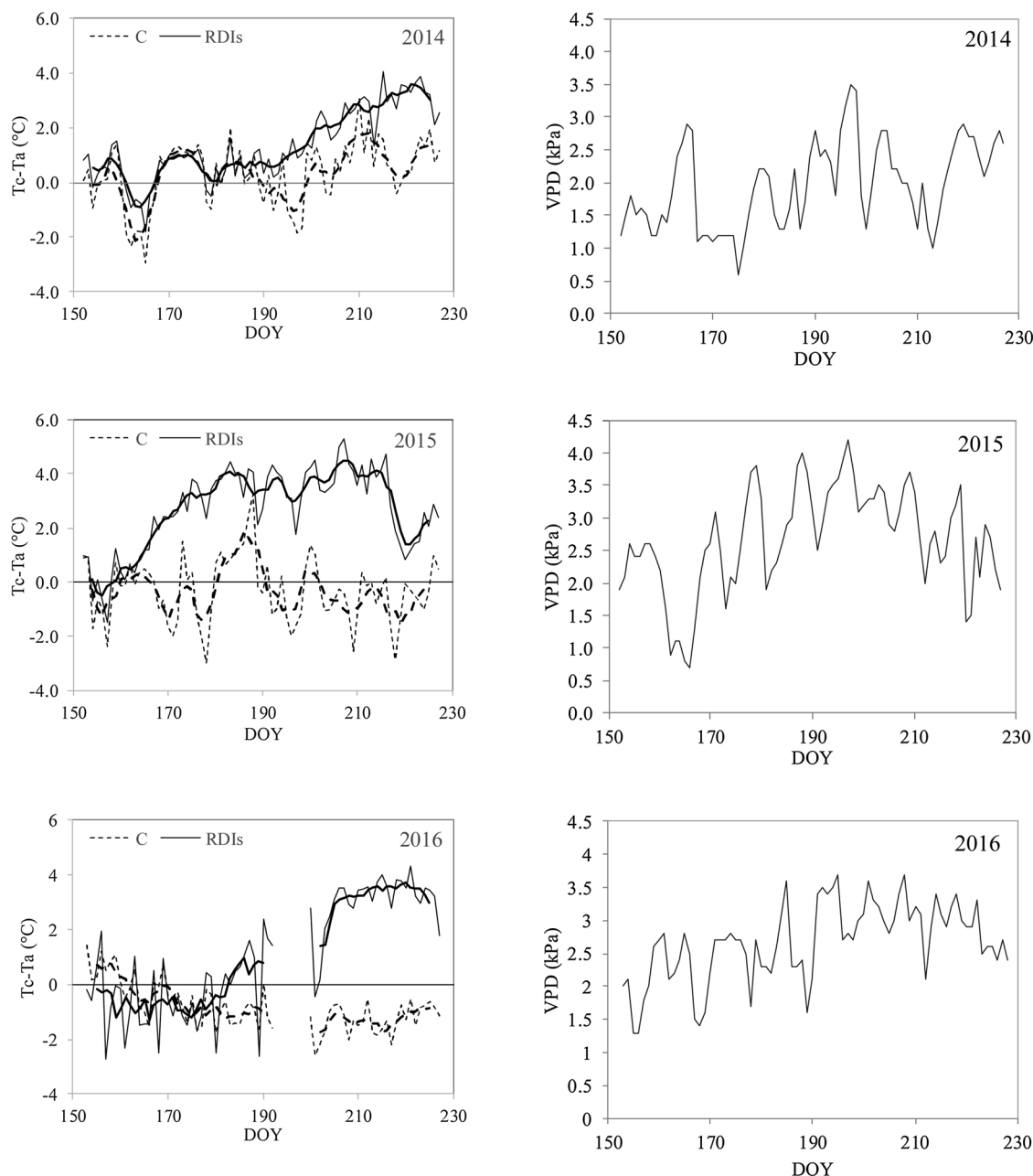
Fig. 2. Time evolution of *Tc-Ta* (°C) at midday for control (thin line, dashed) and RDIs treatment (thin line, solid) for the three years of the study (Left column). Bold lines show the 5-day moving averages. The time course of daily vapor pressure deficit (VPD, kPa) is plotted on the right hand side of the Figure for the three years.
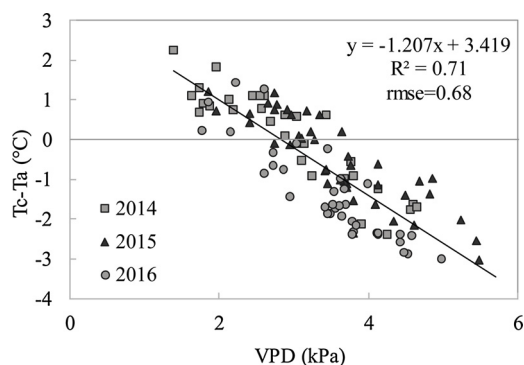

Fig. 3. Relationship between *Tc-Ta* (°C) for control trees and the measured VPD at midday (averaging from 11.00 to 13.00, solar time). Each point corresponded to cloudless daily observations (n = 113).

reaching a minimum close to 0 when the CWSI was close to 1. When the transpiration rate was normalized by the evaporative demand and tree size (kT/GC), it ranged between 1.4 and 0.1 (Fig. 5b). Both regressions (Fig. 5a and b) presented a similar scatter, because of the narrow range of variation of the evaporative demand during the summer in our conditions and the homogeneity in tree size within the orchard.

Water potential and stomatal conductance were also related to the CWSI values obtained around the time of measurement (Fig. 6a and b). The relationship between stem water potential and CWSI adjusted to a second order polynomial regression with a R^2 of 0.80 (Fig. 6a). Water potential was maintained close to maximum values (above -1.2 MPa) until CWSI reached a threshold of 0.2. From this point, the decrease in CWSI values was associated with a decrease in water potential values. Minimum values of SWP were close to -3.3 MPa were associated with CWSI values close to 0.8.

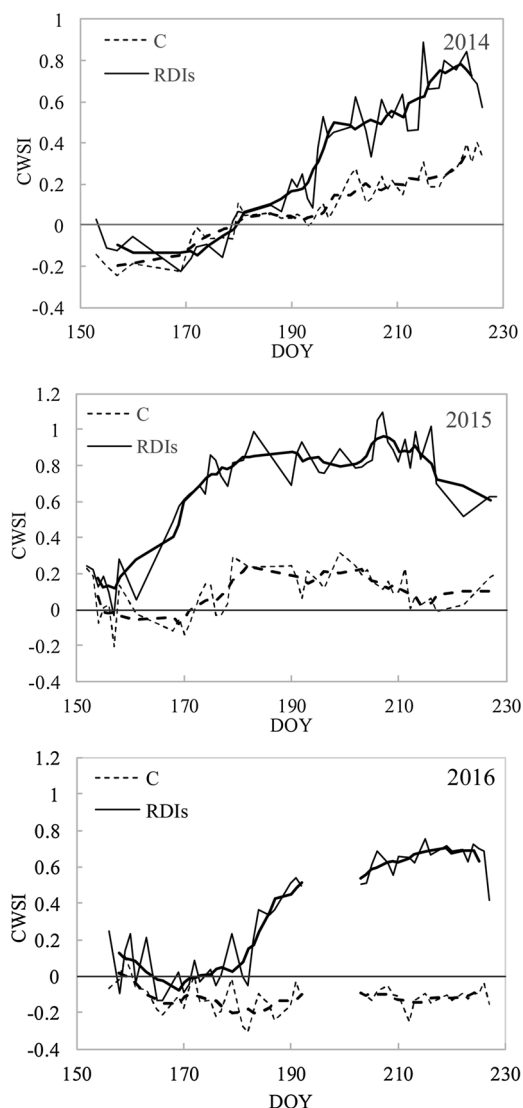The relationship between stomatal conductance and CWSI showed a

Fig. 4. Time course of the Crop Water Stress Index (CWSI) for control (thin line, dashed) and RDIs treatment (thin line, solid) for the three years of the study. Bold lines show the 5-day moving averages.

linear regression with a R^2 ranging 0.88 (Fig. 6b). These results were similar to the relationship observed with the transpiration rate (Fig. 5). In control trees, stomatal conductance reached maximum values of 420 mmol·m^{-2}·s^{-1}, which corresponded with a CWSI close to 0. Minimum Gs values observed were below 100 mmol·m^{-2}·s^{-1}.

Considering the close relationship between thermal data and transpiration observed in this study (Fig. 5), and the relation between transpiration and yield (water production function) that has been developed for almond (López-López et al., 2018b), it can be hypothesized that the average CWSI for the entire season would be related to crop yield. Fig. 7 presents the relationship between nut yield and the average CWSI of the selected trees where the IRT sensors were installed for the period comprised between June and harvest (mid-August), as it was plotted in Fig. 4. Data acquired before June have been discarded from this analysis in order to ensure that no soil background effects on IRT readings were present due to insufficient canopy development. The relation observed in Fig. 7 could be used for empirically estimating water-limited crop yield from thermal-derived CWSI in this orchard.

Taking into account that, in this experiment, water status varied linearly (in the case of the deficit irrigated treatments) or was maintained near constant values (control treatment and trees outside of the experimental design), it was hypothesized that the average CWSI for the whole period could be inferred from canopy thermal observations obtained in two flights performed during the kernel filling period. Aerial thermal imagery acquired in 2014 and 2015 were used to derive an average value of CWSI$_{airborne}$ at the tree level for the whole orchard. For both years, the CWSI$_{airborne}$ was obtained averaging the values for the two flights performed. The yield-CWSI relationship of Fig. 7 in the trees monitored with IRT sensors was used to estimate crop yield at individual tree level from the measured CWSI$_{airborne}$, and the comparative results with actual yields are shown in Fig. 8. There was good agreement between observed and estimated yield data, with an RMSE equal to 1.54 kg/tree.

Finally, the methodology presented here enables the estimation of crop yield derived from thermal imagery. Fig. 9 presents a map of estimated crop yield for the whole orchard (comprising around 850 trees), where the variability associated mainly to watering regimes applied in the experiment can be clearly observed. Values ranged from 3.4 to 17.4 kg/tree, with a mean value for the whole orchard of 9 kg/tree.

4. Discussion

This study demonstrated that thermal information is a valuable tool for monitoring the transpiration rate as well as the water status in almonds. The IRT sensors installed over selected trees allowed the continuous monitoring of canopy temperature during the three years included in this analysis, enabling the accurate assessment of the NWSB, similarly to previous works carried out in other Mediterranean orchard tree crops (Testi et al., 2008; Gonzalez-Dugo et al., 2014; Egea et al., 2017). The NWSB of almonds was similar to that observed in pistachio by Testi et al. (2008).

This study demonstrates the close relationship between the transpiration rate and the thermal-derived CWSI on a daily basis (Fig. 5a).
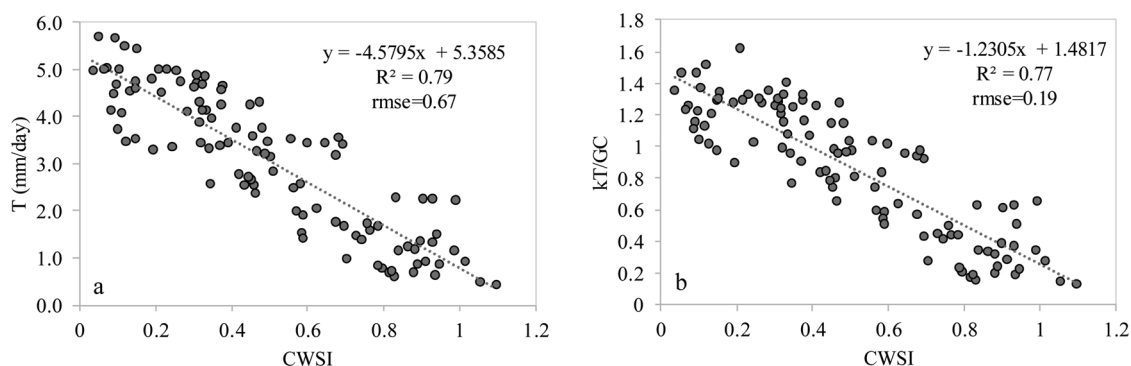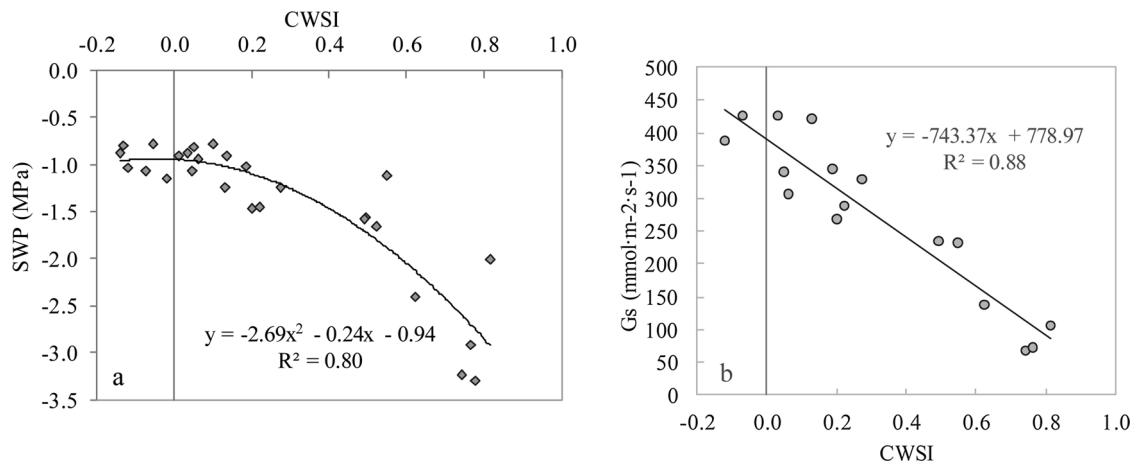

Fig. 5. Relationships between daily CWSI against (a) the transpiration rate; and (b) the ratio between the transpiration coefficient and ground cover (kT/GC, b). Each point corresponds to a single tree. The three years of the study are included in the analysis.

Fig. 6. Relationship between CWSI and stem water potential (MPa; A) and stomatal conductance (Gs; mmol·m^{-2}·s^{-1}; B). Individual measurements performed at midday during the three years of the study were included in the analysis.

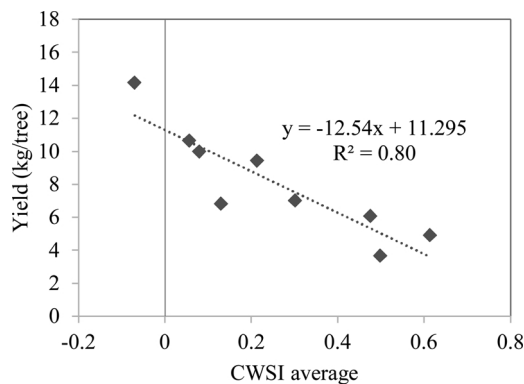**Fig. 7.** Relationship between the estimated average CWSI (obtained from the IRT sensors) and crop yield (kg/tree).

Fig. 9. Interpolated map of predicted yield (kg/tree) in the experimental orchard using Fig. 7 and the CWSI$_{airborne}$. Yield data for 2014 and 2015 are calculated according to the methodology described in the text and the values of the two years were averaged. Experimental plots are indicated in the Figure.
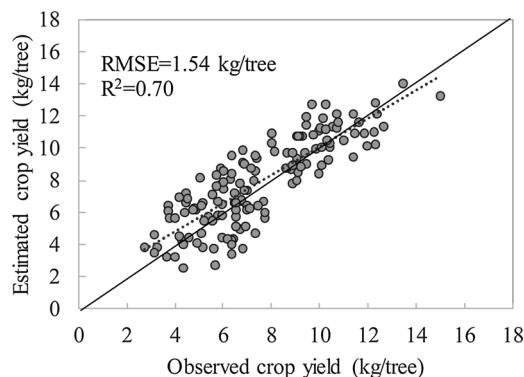

Fig. 8. Relationship between observed and estimated yield (kg/tree). Each point corresponds to a single tree and year. Data from 2014 and 2015 are considered herein (n = 150).

Maximum values of kT/GC (Fig. 5b) ranged between 1.2 and 1.4, which is in agreement with the findings of Espadafor et al. (2015) under well-watered conditions. It is important to note that while CWSI is an instantaneous measurement and was acquired at midday, transpiration rate and kT/GC were calculated on a daily basis. In order to minimize the effects of the two-time scales considered in the relationship, only days under clear sky conditions from sunrise to sunset were included in this analysis, where midday observations are generally representative of integrated daily values. Nevertheless, it is possible that part of the scatter observed in Fig. 5a and b is related to the different time scales of the two variables.
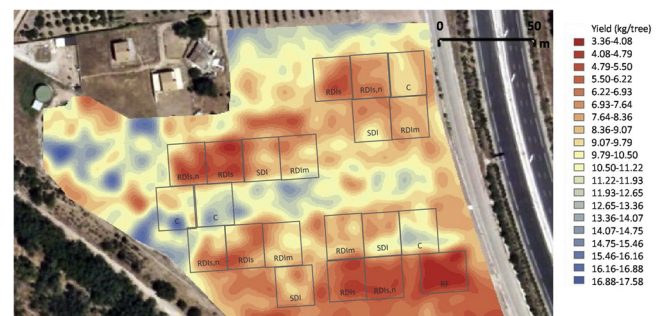
The CWSI also tracked successfully water status, as was demonstrated by the close relationship observed between CWSI and both, water potential and stomatal conductance measured on sunlit leaves (Fig. 6). The relations observed here were similar to those obtained in citrus (Gonzalez-Dugo et al., 2014), although in almonds, the threshold value of CWSI related to a decrease in water potential was 0.2; while in citrus it varied between 0.3 and 0.4. This threshold value of about 0.2 observed in almond was related to a water potential value close to -1.2 MPa. This result agrees with the conclusion obtained by Espadafor et al. (2017) for the same orchard, where for the first time, almond transpiration was assessed under different watering levels. In this study, a value of -1.1 MPa was identified as a threshold for the initial tree transpiration decline. Previous works also observed a good relationship between stomatal conductance, water potential, and even leaf transpiration rate with the CWSI (Xu et al., 2016; Egea et al., 2017). Egea et al. (2017) also reported a better correlation of CWSI to stomatal conductance, compared to water potential, which is in agreement with the control of the transpiration rate exerted by the stoma under water stress (Jones, 1998).

The time evolution of CWSI clearly followed the water application rate in the two treatments monitored with IRT sensors. Control trees displayed an average value of CWSI close to 0, which is expected considering that these trees were used to derive the NWSB. Water application in treatment RDIs during kernel filling was substantially decreased, down to 15–20% of control trees. As a consequence, the CWSI sharply increased after the beginning of the stress period. Although the soil in this experiment is deep and with a relatively high water holding capacity (López-López et al., 2018a), the shortage of water application resulted in an increase of CWSI to maximum values between 0.7 and 0.9

at the end of the kernel filling period (variable for the three years of the study).

Recently, López-López et al. (2018b) developed the water production function for hard shelled almonds. This function relates the seasonal transpiration to crop yield. Under the local conditions of the experiment described here, the relationship between the seasonal course of CWSI and transpiration, together with the water production function, could serve as a basis for the estimation of crop yield. Irmak et al. (2000), and recently Han et al. (2018), described the relationship between the seasonal average CWSI and yield in maize. Instead of considering the whole season, this study was focused on the period comprised between June and August, because of the lack of accuracy of the IRT sensors to monitor the canopy temperature when the leaf area has not been fully developed. The rationale behind this hypothesis is that, considering that all trees were managed similarly during all the postharvest periods and the strong effect of water stress during the kernel filling stage on yield (as shown by Goldhamer et al., 2006; Egea et al., 2010; Goldhamer and Fereres, 2017), the monitoring of canopy temperature during this critical period might provide accurate estimations of crop yield. Our results of Fig. 8 appear very promising, although more research is needed to assess the robustness of the relationship depicted in Fig. 7.

The CWSI$_{airborne}$ calculated for every tree in the orchard was used to estimate final yield, under the assumption that the average value of CWSI$_{airborne}$ for two flights is related to the average CWSI for the whole period. The comparison between measured and estimated crop yield, comprising 80 trees and two years, obtained good results. It displayed an overall good performance for this experimental site under the Mediterranean conditions. The ability for estimating crop yield from a limited number of aerial thermal data acquisitions will be related to the variability in the water stress patterns. If this pattern is rather stable and similar to the one developed here, an average CWSI value can be used to estimate crop yield in the context of precision agriculture. According to this premise, the CWSI$_{airborne}$ calculated in this study successfully tracked crop yield because the water stress pattern during kernel filling did not change abruptly, but it showed a smooth decline or steadiness, and also because there were no differences in crop management during the postharvest period, which may severely affect subsequent crop yield, as was observed by Goldhamer et al. (2006). If water status oscillates as a consequence of the irrigation schedule (such as in the case of low frequency irrigation systems), this approach might not be longer useful as well. Under intermittent watering conditions, more frequent flights would be needed to improve the time resolution of the water status, and through a time-integration technique, to obtain a time-averaged CWSI that would be representative for the monitoring period. With these premises the proposed model would be more generally applicable and robust when used with aerial remote sensing data. This kind of information can be very valuable for assessing thresholds of water status related to crop yield loss during the season. The link with the airborne thermal imagery enables the estimation of the spatial distribution of crop yield in the orchard as a function of water status, which is of interest in the context of precision agriculture. It may provide information, not only for water management, but also, for the analysis of economic aspects related with nutrient or pesticide applications. The extensive use of airborne imagery for precision agriculture, in combination with the development of sensors at the tree level, such as the sap flow sensors, offers a wide range of possibilities for optimizing water use and crop yield in irrigated agriculture.

5. Conclusions

This paper demonstrates that CWSI is a suitable indicator of almond water status during summertime under semiarid conditions. A stable NWSB was obtained from IRT sensors measuring tree temperatures for three years for the development of the CWSI. The CWSI was found to be closely related to transpiration measured on individual trees with sap flow sensors. Good results were also obtained in the relationship of CWSI with water potential and stomatal conductance, as has been observed previously for other crops. The relationship between CWSI and transpiration during the kernel filling period displayed overall good results, allowing the linkage between average CWSI and yield. Furthermore, the gradual variation of water status during the experiment enabled the extrapolation of the model to the CWSI$_{airborne}$, calculated after the thermal imagery acquired with a manned vehicle over the experimental site. The model relating yield to CWSI$_{airborne}$ yielded good results, with a RMSE of 1.54 kg/tree. More research is needed to determine the validity of this approach in other climates, growing conditions, and irrigation management.

References

Bellvert, J., Marsal, J., Girona, J., Gonzalez-Dugo, V., Fereres, E., Ustin, S., Zarco-Tejada, P., 2016a. Airborne thermal imagery to detect the seasonal evolution of crop water status in Peach, nectarine and Saturn peach orchards. Remote Sens. 8, 39.

Bellvert, J., Zarco-Tejada, P., Narsal, J., Girona, J., Gonzalez-Dugo, V., Fereres, E., 2016b. Vineyard irrigation scheduling based on airborne thermal imagery and water potential thresholds. Aust. J. Grape Wine Res. 22 (2), 307–315.

Berni, J.A.J., Zarco-Tejada, P.J., Suarez, L., Fereres, E., 2009. Thermal and narrowband multispectral remote sensing for vegetation monitoring from an unmanned aerial vehicle. Ieee Trans. Geosci. Remote. Sens. 47 (3), 722–738.

Egea, G., Nortes, P.A., Gonzalez-Real, M.M., Baille, A., Domingo, R., 2010. Agronomic response and water productivity of almond trees under contrasted deficit irrigation regimes. Agric. Water Manag. 97, 171–181.

Egea, G., Padilla-Diaz, C.M., Martinez-guanter, J., Fernandez, J.E., Perez-Ruiz, M., 2017. Assessing a crop water stress index derived from aerial thermal imaging and infrared thermometry in super-high density olive orchards. Agric. Water Manag. 187, 210–221.

Espadafor, M., Orgaz, F., Testi, L., Lorite, I.J., Villalobos, F.J., 2015. Transpiration of young almond trees in relation to intercepted radiation. Irrig. Sci. 33 (4), 265–275.

Espadafor, M., Orgaz, F., Testi, L., Lorite, I., Gonzalez-Dugo, V., Fereres, E., 2017. Responses of transpiration and transpiration efficiency of almond trees to moderate water deficits. Sci. Hortic. 225, 6–14.

Fereres, E., Soriano, M.A., 2007. Deficit irrigation for reducing agricultural water use. J. Exp. Bot. 58 (2), 147–159.

Fereres, E., Goldhamer, D., Sadras, V.O., 2012. Yield response to water of fruit trees and vines: guidelines. In: Steduto, P., Hsiao, T.C., Fereres, E., Raes, D. (Eds.), Crop Yield Response to Water. Irrigation and Drainage Paper. Food and Agriculture Organization of the United Nations (FAO), Rome, pp. 246–296.

Goldhamer, D., Fereres, E., 2017. Establishing an almond water production function for California using long-term yield response to variable irrigation. Irrig. Sci. 35, 169–179.

Goldhamer, D.A., Viveros, M., Salinas, M., 2006. Regulated deficit irrigation in almonds: effects of variations in applied water and stress timing on yield and yield components. Irrig. Sci. 24 (2), 101–114.

Gonzalez-Dugo, V., Zarco-Tejada, P., Nicolas, E., Nortes, P.A., Alarcon, J.J., Intrigliolo, D.S., Fereres, E., 2013. Using high resolution UAV thermal imagery to assess the variability in the water status of five fruit tree species within a commercial orchard. Precis. 14, 660–678.

Gonzalez-Dugo, V., Zarco-Tejada, P.J., Fereres, E., 2014. Applicability and limitations of using the crop water stress index as anindicator of water deficits in citrus orchards. Agric. For. Meteorol. 198-199, 94–104.

Han, M., Zhang, H., DeJonge, K.C., Comas, L.C., Gleason, S., 2018. Comparison of three crop water stress index models with sap flow measurements in maize. Agric. Water Manag. 203, 366–375.

Hsiao, T.C., 1973. Plant responses to water stress. Annu. Rev. Plant Physiol. 24, 519–570.

Idso, S.B., Jackson, R.D., Pinter, P.J.J., Reginato, R.J., Hatfield, J.L., 1981. Normalizing the stress degree-day parameter for environmental variability. Agric. Meteorol. 24, 45–55.

Irmak, S., Haman, D.Z., Bastug, R., 2000. Determination of crop water stress index for irrigation timing and yield estimation of corn. Agron. J. 92, 1221–1227.

Jackson, R., Idso, S., Reginato, R., Pinter, P.J., 1981. Canopy temperature as a crop water stress indicator. Water Resour. Res. 17, 1133–1138.

Jones, H.G., 1998. Stomatal control of photosynthesis and transpiration. J. Exp. Bot. 49, 387–398.

Jones, H.G., Stoll, M., Santos, T., Sousa, C.D., Chaves, M.M., Grant, O.M., 2002. Use of infrared thermography for monitoring stomatal closure in the field: application to grapevine. J. Exp. Bot. 53 (378), 2249–2260.

López-López, M., Espadafor, M., Testi, L., Lorite, I.J., Orgaz, F., Fereres, E., 2018a. Water use of irrigated almond trees when subjected to water deficits. Agric. Water Manag. 195, 84–93.

López-López, M., Espadafor, M., Testi, L., Lorite, I.J., Orgaz, F., Fereres, E., 2018b. Yield response of almond trees to transpiration deficits. Irrig. Sci. 36 (2), 111–120.

Maes, W.H., Steppe, K., 2012. Estimating evapotranspiration and drought stress with ground-based thermal remote sensing in agriculture: a review. J. Exp. Bot. 63 (13), 4671–4712.

Naor, A., Birger, R., Peres, M., Gal, Y., Elhadi, F.A., Haklay, A., Assouline, S., Schwartz, A., 2017. The effect of irrigation level in the kernel dry matter accumulation period on almond yield, kernel dry weight, fruit count, and canopy size. Irrig. Sci. 1–8.

O'Shaughnessy, S.A., Andrade, M.A., Evett, S.R., 2017. Using an integrated crop water stress index for irrigation scheduling of two corn hybrids in a semi-arid region. Irrig. Sci. 35, 451–467.

Romero, P., Botia, P., Garcia, F., 2004. Effects of regulated deficit irrigation under sub-surface drip irrigation conditions on water relations of mature almond trees. Plant Soil 260 (1-2), 155–168.

Tanner, C.B., Sinclair, T.R., 1983. Efficient water use in crop production: research or research. In: Taylor, Howard M. (Ed.), Limitations to Efficient Water Use in Crop Production. ASA, Madison, pp. 1–27.

Testi, L., Villalobos, F.J., 2009. New approach for measuring low sap velocities in trees. Agric. For. Meteorol. 149, 730–734.

Testi, L., Goldhamer, D., Iniesta, F., Salinas, M., 2008. Crop water stress index is a sensitive water stress indicator in pistachio trees. Irrig. Sci. 26, 395–405.

Turner, D., Lucieer, A., Watson, C., 2012. An automated technique for generating georectified mosaics from ultra-high resolution unmanned aerial vehicle (UAV) imagery, based on structure from motion (SfM) points clouds. Remote Sens. (Basel) 4, 1392–1410.

Xu, J., Lv, Y., Liu, X., Dalson, T., Yang, S., Wu, J., 2016. Diagnosing crop water stress of rice using infrared thermal imager under water deficit condition. Int. J. Agric. Biol. 18, 565–572.

Zarco-Tejada, P.J., Gonzalez-Dugo, V., Berni, J.A.J., 2012. Fluorescence, temperature and narrow-band indices acquired from a UAV platform for water stress detection using a micro-hyperspectral imager and a thermal camera. Remote Sens. Environ. 117, 322–337.